03 Sep 2020

The Influence of Ti, Nb and V on the Hot Ductility of As-Cast Microalloyed Steels

Madhuri Varadarajan

Laura Bartlett
Missouri University of Science and Technology, lnmkvf@mst.edu

Ronald J. O'Malley
Missouri University of Science and Technology, omalleyr@mst.edu

Semen Naumovich Lekakh
Missouri University of Science and Technology, lekakhs@mst.edu

Recommended Citation

M. Varadarajan et al., "The Influence of Ti, Nb and V on the Hot Ductility of As-Cast Microalloyed Steels," *Proceedings of the AISTech 2020 (2020, Cleveland, OH)*, pp. 1470-1478, Association for Iron & Steel Technology (AIST), Sep 2020.
The definitive version is available at https://doi.org/10.33313/380/158

AISTech 2020 — Proceedings of the Iron & Steel Technology Conference
DOI 10.33313/380/158

The Influence of Ti, Nb and V on the Hot Ductility of As-Cast Microalloyed Steels

Madhuri Varadarajan[1], Laura N. Bartlett[1], Ronald J. O'Malley[1], Simon N. Lekakh[1]

[1]Peaslee Steel Manufacturing Research Center, Missouri University of Science and Technology,
1400 North Bishop Avenue, Missouri, United States, 65409-0340
Phone: 573-341-4711
Email: lnmkvf@mst.edu

ABSTRACT

Microalloying with Ti, Nb and V, both individually and in combination, is a common method for producing steels with high strength and toughness. However, interaction with other elements and impurities can lead to cracking during continuous casting and rolling. The hot ductility of commercially cast V, Nb and Nb-V-Ti steels has been investigated using two experimental methods: tensile testing utilizing a servo-hydraulic load frame with a resistance furnace and thermomechanical testing using rapid joule heating. The temperature-dependent ductility of these steels is compared for both test methods. Factors that influence the ductility of these steels are discussed.

Keywords: Microalloyed steel, hot ductility, surface cracks, hot tensile tests

INTRODUCTION

One of the main problems faced in continuous casting is the formation of transverse cracks. Transverse cracks are surface or near surface cracks in the cast slab that are oriented perpendicular to the direction of casting. These cracks are often associated with oscillation marks and they can penetrate to a depth of 5-8mm or more below the surface of the slab. The cracks often originate in the straightening region of the caster on the top surface of the slab when unbending occurs at temperatures of 700-1000°C where the steel is known to exhibit low ductility. This "ductility trough" can be observed in hot tensile tests by measuring the % reduction of area (%RA) at specimen failure. Carbon steels generally exhibit three regions of low ductility. A high temperature ductility trough exists at temperatures near the solidus temperature where liquid is still present. In the high temperature low ductility range, ductility depends on segregation of alloying elements and impurities that produce a low melting point liquid that is associated with hot tearing. The second ductility trough exists in a temperature range from 900 to 1200°C in austenite. In this temperature range oxides, sulphides, carbonitrides, and other fine precipitates formed at austenite grain boundaries can reduce ductility. Precipitation on austenite grain boundaries can lead to precipitate free zones adjacent to the grain boundary that create localized weakening in this area, producing low ductility intergranular failure [1]. The third ductility trough exists in the temperature range from 600-900°C near the Ar_3 temperature. In this region ferrite films are formed at austenite grain boundaries. Below the Ar_3 temperature, the amount of ferrite increases, and ductility increases. In addition, the solubility of carbides, nitrides and carbonitrides is lower in ferrite than in austenite, promoting precipitation in the ferrite film. Thus, the cause of the ductility trough in this temperature range is a combination of ferrite films on grain boundaries as well as microalloy carbide, nitride and complex carbonitride precipitates [2, 3].

To avoid high production costs and yield losses on finished products, it is important that defects in continuous cast slabs are minimized. The hot ductility of steel is highly dependent on the presence of microalloying elements such as Nb, V and Ti [4]. Optimal use of microalloying elements, such as Ti, Nb, and V, can produce steels that exhibit high strength and toughness when appropriate thermomechanical processing is employed [5-7]. Unfortunately, these elements can sometimes lead to increased susceptibility to transverse cracking.

Niobium has been shown to have a strong effect on the hot ductility of steels, deepening the "ductility trough" and extending the low ductility region to higher temperatures. Mintz, et. al., and Sricharoenchai, et. al., suggest that this is mainly due to the formation of Nb(C, N) precipitates which can retard recrystallization and form precipitates on austenite grain boundaries. Nb additions from 0.017% up to 0.074% were shown to have an effect on ductility [2, 10-12]. Al additions to Nb containing steels were also shown to deepen and widen the ductility trough [2, 13].

Vanadium and titanium have also been shown to affect transverse crack sensitivity. At high nitrogen levels (90-120ppm), vanadium has been reported to cause transverse cracking but below 50 ppm, transverse cracking was not observed [8]. High nitrogen levels favor the precipitation of V(C, N) or VN, but vanadium levels below 0.07% have been reported to inhibit the drop in ductility [9]. Ti additions of 0.015-0.04% Ti have also been reported to decrease crack sensitivity by forming coarse TiN, thereby reducing the formation of fine AlN and Nb(C,N) precipitates [14,15]. Mintz, et. al., reported that Ti additions can maintain a fine austenite grain size during heat treatment due to the grain boundary pinning effects by TiN precipitates which are stable at high temperatures [16]. However, the benefits were not evident in the continuously cast steels.

The objective of the present research is to investigate the influences of Ti, Nb and V on the hot ductility of three as-cast microalloyed steel slabs received from industry. This paper focuses on the use of two laboratory hot tensile test methods, one using a servo hydraulic load frame equipped with resistive heating furnace and one using a custom built joule heating apparatus equipped with an electro-mechanical tensioning cylinder. Tensile samples taken from the as-cast steel slabs were reheated, soaked, cooled to temperature, and tested to failure to determine the reduction of area (%RA) of the specimen. The two test methods are compared and factors influencing the ductility of these steels are discussed. In future work, these testing methods will also be compared to a proposed new hot bending test method that will be capable of directly observing crack initiation on an as-solidified and cooled specimen.

EXPERIMENTAL METHOD

Materials and composition

Steel slab samples with compositions shown in Table 1 were supplied by United States Steel Corporation. Samples for hot tensile testing were cut from 203mm thick, as-cast slab samples from the locations shown in Figure 1. The hot ductility samples were prepared so that the tensile specimen orientation was perpendicular to the columnar grain structure of the as-cast slab to ensure that testing was performed perpendicular to the direction of solidification in the slab. Care was taken when cutting of the samples to avoid centerline segregation, internal crack sites, and the narrow face edges of the as-cast slab. The heat affected regions from the oxy-acetylene torch cuts were avoided during preparation of the tensile samples.

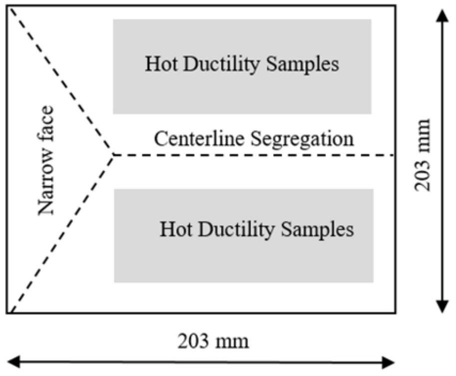

Figure 1. Position of hot ductility samples taken from as-cast steel slab.

Optical emission arc spectroscopy analysis was performed along the length of the slab and the average chemical composition of the steels, reported in wt. %, are given in Table 1. Leco combustion and inert gas fusion analysis were used to determine the composition of carbon, sulphur and nitrogen levels in the steels. The three steels studied are aluminum deoxidized steels with varying levels of carbon ranging from low to medium carbon content range with varying amounts of microalloying elements of V, Nb and Ti.

Table 1 Chemistry of the slab section in wt. % as determined by optical emission arc spectroscopy and Leco combustion and inert gas fusion analysis

	C*	Si	Mn	P	S*	Al	V	Nb	Ti	N** (ppm)
V Steel	0.175	0.03	0.64	0.02	0.007	0.046	0.061	-	0.002	42
Nb-Ti Steel	0.102	0.03	1.11	0.02	0.017	0.037	-	0.026	0.018	76
V-Nb-Ti Steel	0.090	0.21	1.20	0.02	0.011	0.031	0.045	0.040	0.023	60

* - Leco CS600 Analyzer, ** - TC 500 N/O Analyzer

The V steel had a somewhat higher carbon content than the Nb-Ti and V-Nb-Ti steel with 0.06%V and a residual Ti of 0.002%. The Nb-Ti steel had a higher Mn and S content than the V steel and contained 0.026% Nb and 0.018% Ti. The V-Nb-Ti steel had similar Mn and S levels to the Nb-Ti steel, but contained 0.023% Ti and 0.04% Nb and V. All three steels studied had nitrogen levels that ranged from 42 to 76 ppm.

Experimental determination of hot ductility of steels

Several different experimental techniques are being applied in this research for measuring the hot ductility of steels in the temperature range associated with transverse crack formation during continuous casting. The methods being reported here involve the reheating of as-cast slab samples to re-dissolve the microalloy precipitates (where possible) and then cooling to the desired test temperature and applying a controlled displacement at a controlled strain rate while measuring the load to failure. In future work, a test procedure that directly tests the as-solidified and cooled steel is planned. In this paper, the hot ductility of commercially cast V, Nb-Ti and V-Nb-Ti steels has been investigated using two experimental methods: (1) tensile testing utilizing a servo-hydraulic load frame with a resistance furnace and (2) custom built thermomechanical testing apparatus that uses rapid joule heating with a electro-mechanically controlled tensioning system. Figure 2 (a) shows a schematic temperature profile used for the hot tensile tests, which were performed using the servo-hydraulic load frame with the resistance furnace. The samples were prepared according to the ASTM E8-16a standard. Small round sub-size specimens were used. The thermomechanical cycle used in this study was as follows: the specimens were heated at 1°C/s to 1200°C in argon atmosphere using a resistance furnace and then were held for 2 min for dissolution of precipitates. Subsequently, the samples were cooled to the test temperature in the range of 650-900°C at a cooling rate of 1°C/s. Samples were held at the test temperature for 2 min. They were strained to failure at a constant strain rate of 3 x 10^{-3}/s which was selected to approximately match the strain rate during the straightening operation of the continuous casting process. After failure, the samples were allowed to cool to room temperature.

The rapid joule heating system uses a mechanical loading assembly with an inline drive (10 kN max), a load cell (0.5N resolution) and laser displacement sensor (±1 µm resolution). A 400 amp DC joule heater is used to heat the samples and an IR camera (1 mm spot size, ±1 °C) monitors the temperature of the sample. The system uses LabView software to monitor and control tests and temperature cycles by appropriate feedback control. Figure 2 (b) shows a schematic temperature profile for the hot tensile tests using joule heating. The samples are flat specimens, typically 96 x 23 mm in cross section. The samples were heated at 5°C/s up to 1200°C using a DC joule heater and then soaked for 2 min. The sample is placed inside a chamber with a continuous flow of argon throughout the test cycle to avoid oxidation of the samples. The samples are cooled to the test temperature in the range of 650-900°C at a cooling rate of 4°C/s. The samples were soaked in the test temperature for 2 min and then strained to failure using a constant strain rate of 3 x 10^{-3}/s and after failure the samples were cooled rapidly to the room temperature. Both test methods employ the same testing parameters except for the differences in the heating and cooling rates. The effect of the different thermal cycles from the two testing methods, particularly the effects of fast vs. slow heating and cooling, on the hot ductility results are presented and discussed.

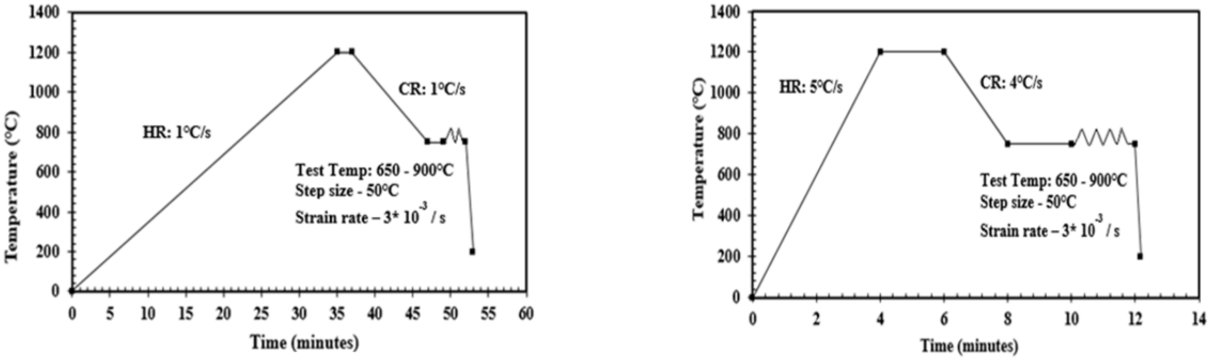

(a) (b)

Figure 2. Schematic diagrams showing the thermal cycles studied. (a) Servo-hydraulic load frame with a resistance furnace (b) Joule resistive heating

Thermodynamic modeling and metallographic analysis

Thermodynamic modeling was performed using FactSage v7.2 to better understand the sequence of phase transformations and precipitation that is expected to occur during solidification and cooling. A prior austenite grain size analysis was also performed to investigate the effect of this variable on the hot ductility of the steels. Samples for grain size analysis were sectioned perpendicular to the columnar grain structure and they were soaked at different times in the γ-α region based on the predicted ferrite-austenite transformation temperature and then rapidly quenched to facilitate austenite grain size measurement. Grain size measurements were performed using the linear intercept method of optical microscopy.

RESULTS AND DISCUSSION

Stress – strain behavior and hot ductility curves of V microalloy steel

Figure 3 a) shows the engineering stress – engineering strain curves of V microalloy steel obtained from the servo -hydraulic load frame (MTS load frame) equipped with electric furnace and Figure 3 b) shows the engineering stress – engineering strain curves from the joule heating experiment. As expected, in both tests the strength decreases with an increase in temperature. There is an abrupt drop in the stress-strain curves from MTS load frame observed at temperatures of 850°C and 900°C (indicated by arrows) which may be evidence of dynamic recrystallization. After 850°C, the curve from both test methods displayed increasing ductility as indicated by larger plastic deformation seen in the stress-strain curve.

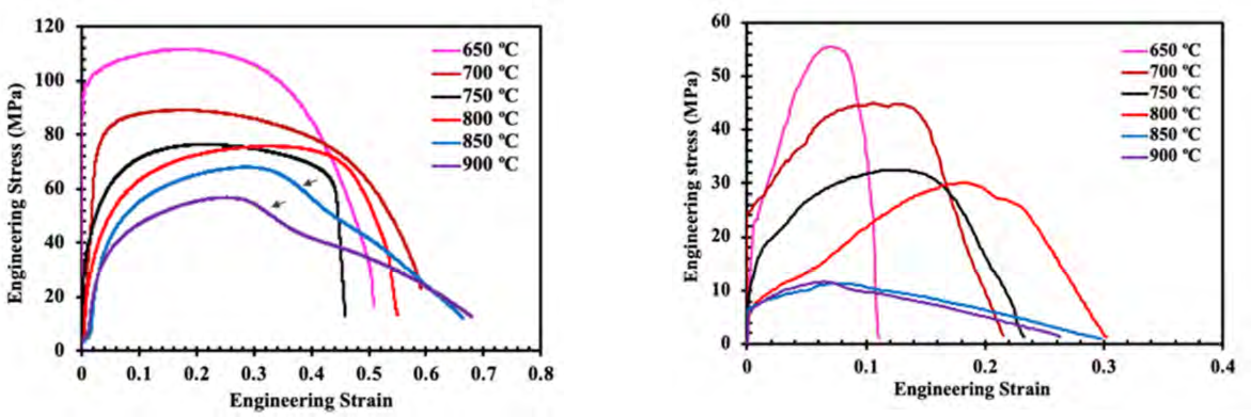

(a) (b)

Figure 3. Engineering stress- engineering strain curves of vanadium microalloy steel at different temperatures a) MTS load frame b) Joule resistive heating.

Figure 4 a) shows the %RA as function of temperature for V microalloy steels from both test methods. The % RA varied from 37% - 97% for the temperatures from 650°C - 900°C and a ductility trough was obtained from the MTS load frame. In joule resistive heating, the %RA varied from 42% - 97%. A minimum drop in ductility was observed from temperature ranges of 700°C - 800 °C.

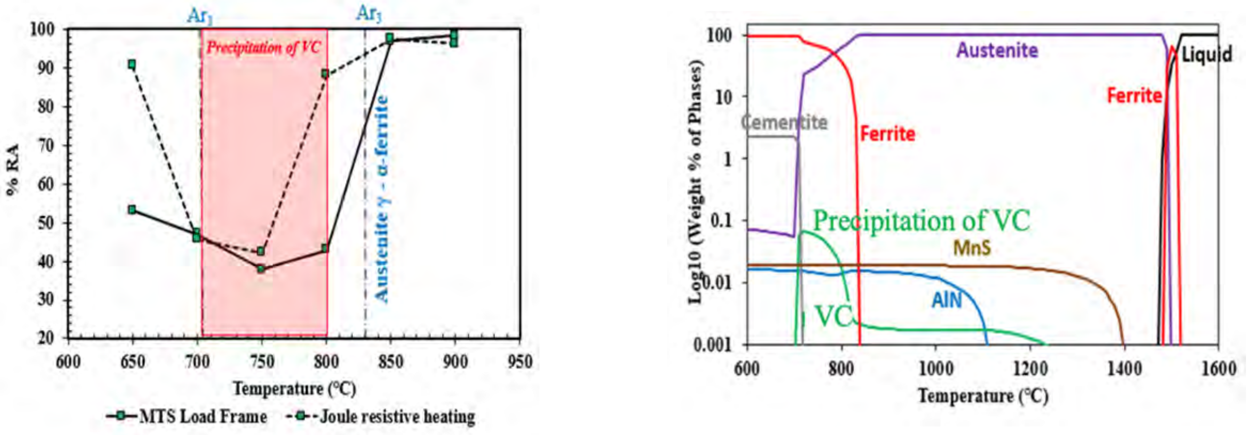

(a) (b)

Figure 4. a) Hot ductility curves of vanadium microalloy steel from both test methods b) Thermodynamic modeling showing precipitation of vanadium carbides from 700°C - 800°C.

Comparing ductility troughs from two test methods, the minimum ductility for both methods was observed at 750℃ with an %RA of around 37% for the MTS load frame test and 42% for the Joule resistive heating test. The 800℃ - 700℃ temperature range where low ductility is observed closely match the temperature for the formation of ferrite and corresponding increased precipitation of vanadium carbide in ferrite predicted by thermodynamic modeling, as shown in Figure 4 b). The ductility drop of the steel is likely related to the intergranular failure along the austenite grain boundaries due to the formation of thin films of ferrite below Ar_3 that allows strain concentrations to build up along the austenite grain boundaries, promoting void formation. Carbide precipitates also form in the ferrite, further reducing the ductility of the steel.

Stress – strain behavior and hot ductility curves of Nb-Ti microalloy steel

Figure 5 shows the engineering stress – engineering strain curves obtained from a) the MTS load frame and b) joule resistive heating tests. Both the test methods showed that with increase in temperature there was a drop in the strength of the steels as expected. The % RA varied from 55% - 98% for temperature ranges from 650℃ - 900℃ in MTS load frame test while in joule resistive heating test, the % RA varied from 59%-98% as shown in Figure 8(a). Both the test methods showed a minimum in ductility at 800℃ with %RA around 55% (MTS load frame) and 59% (Joule resistive heating) which again was close to the austenite to ferrite transformation temperature predicted by thermodynamic modeling.

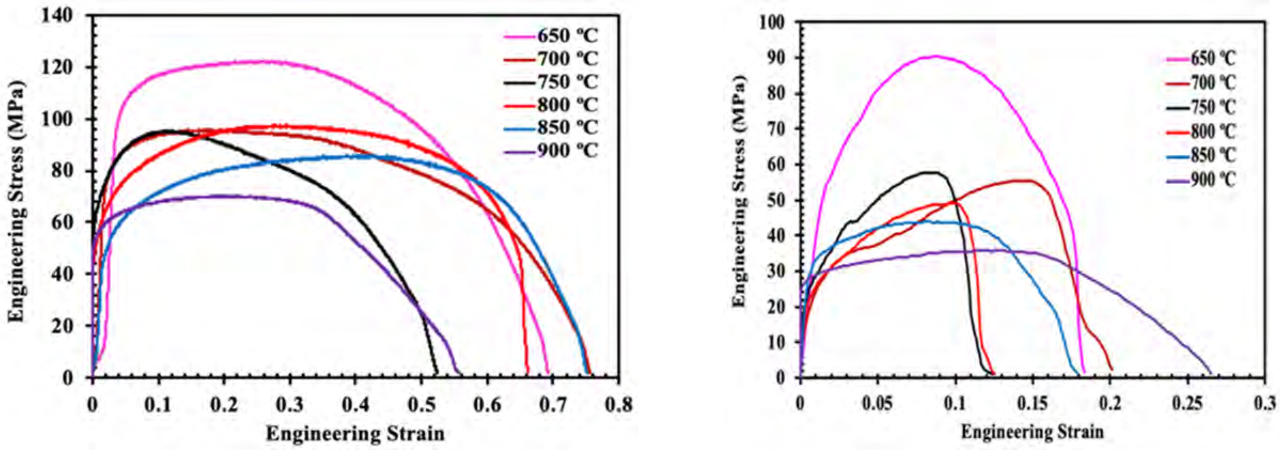

(a) (b)

Figure 5. Engineering stress- engineering strain curves of Nb -Ti microalloy steel at different temperatures a) MTS load frame b) Joule resistive heating.

Figure 6 (b) shows the equilibrium solidification and cooling predictions for this alloy. Equilibrium modeling showed that TiN precipitates form just below the liquidus and during solidification, starting from 1490℃. On the other hand, (Nb,Ti)(C,N) was shown to precipitate in the temperature range from 1100℃-700℃ and AlN precipitation was predicted below 980℃ as shown in Figure 8(b). The temperature at which the ductility starts to drop corresponds closely with the Ar_3 transformation temperature of the alloy. The predicted formation of (Nb,Ti)(C,N) at higher temperatures, shown in Figure 6(a), does not appear to negatively impact the ductility of the alloy.

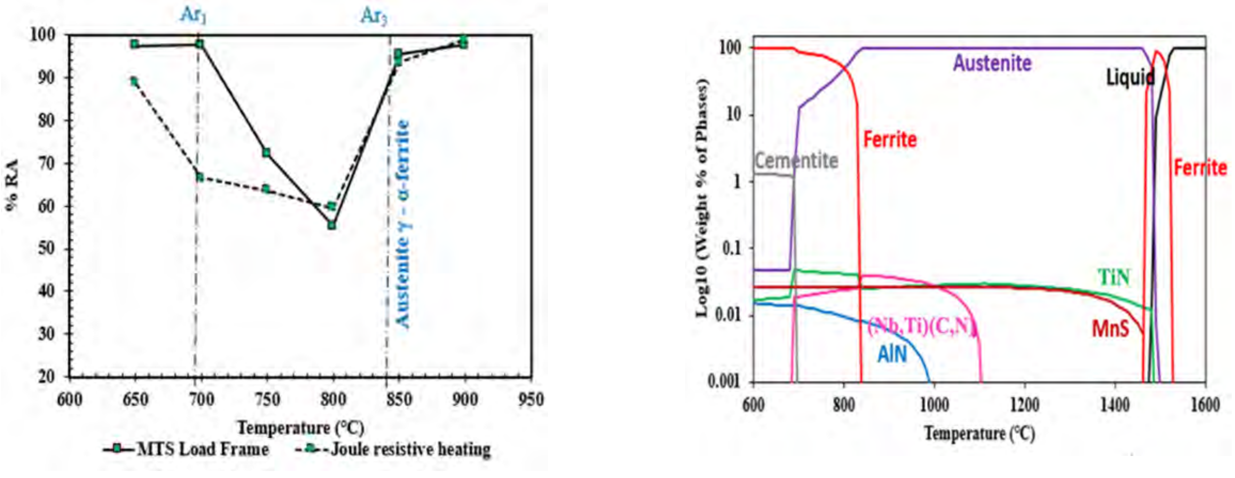

(a) (b)

Figure 6. a) Hot ductility curves of Nb-Ti microalloy steel from both test methods b) Thermodynamic modeling showing precipitation of TiN from the liquid just after the liquidus and (Nb,Ti)(C,N) formation after solidification from 700 -1100 °C.

Stress – strain behavior and hot ductility curves of V-Nb-Ti microalloy steel

Figure 7 shows the engineering stress – engineering strain curves obtained from a) MTS load frame test and b) joule resistive heating test. Both the test methods showed that with increase in temperature there was a drop in the strength of the steels. The % RA varied from 60% - 98% for temperature ranges from 650°C - 900°C in MTS load frame while in joule resistive heating, the % RA varied from 69%-95% as shown in Figure 8(a). The ductility drop was observed at 800°C with %RA around 60% in MTS load frame while in joule resistive heating, ductility drop was observed at 750°C with % RA around 69%.

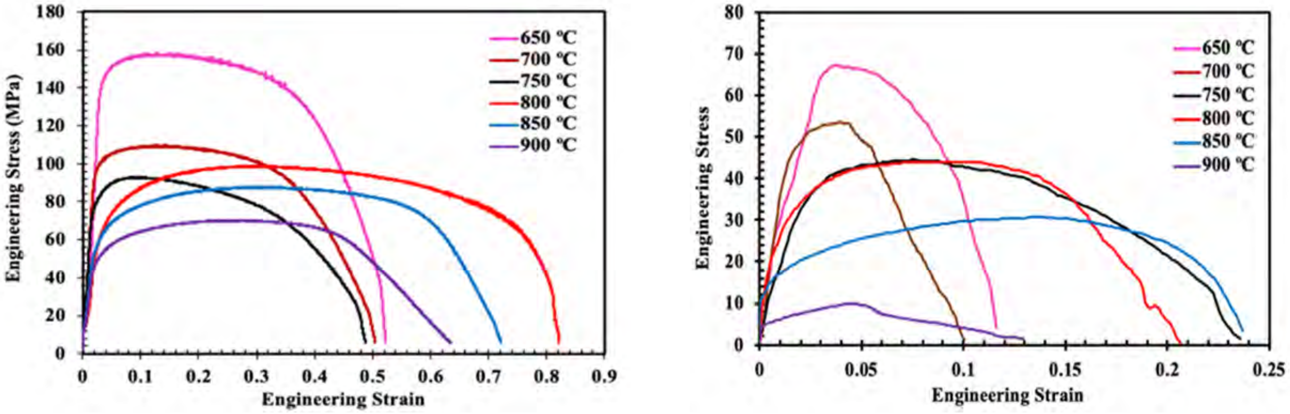

(a) (b)

Figure 7. Engineering stress- engineering strain curves of V- Nb -Ti microalloy steel at different temperatures a) MTS load frame b) Joule resistive heating.

Figure 8 (b) shows the equilibrium solidification and cooling predictions for this alloy. Equilibrium modeling predicts that TiN precipitates below the liquidus temperature during solidification, starting below 1500°C. The addition of Ti appears to result in an improvement of the hot ductility of this steel under the conditions of this test. Since the steels were solution treated at 1200°C, TiN or Ti rich precipitates which form from the liquidus are not completely dissolved at the solution treating temperatures. However, their presence does not appear to negatively impact the hot ductility of the steel at high temperatures. The ductility drop, as observed between 750°C-800°C is closer to the Ar_3 transformation temperature of the alloy.

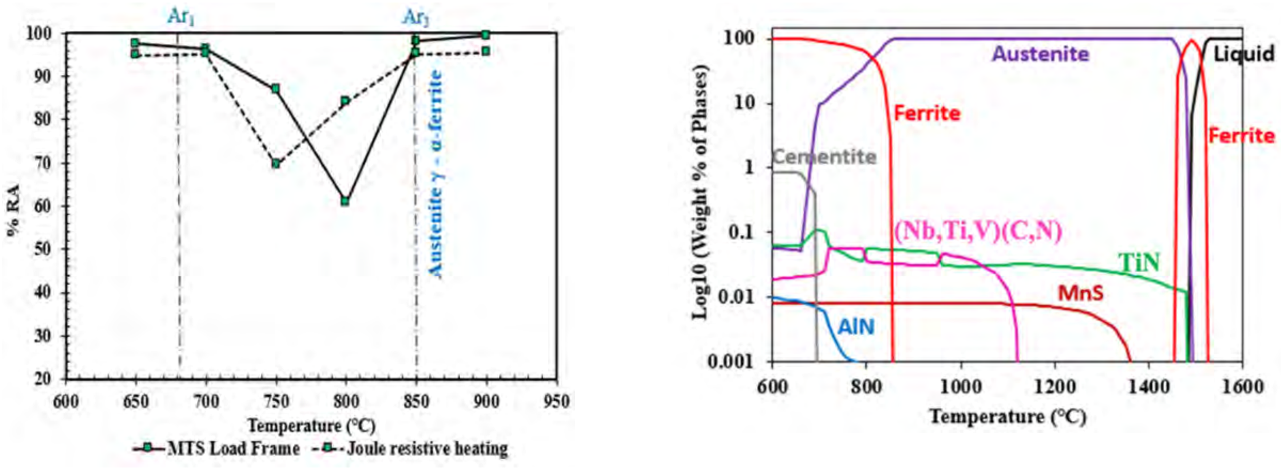

(a) (b)

Figure 8. a) Hot ductility curves of V-Nb-Ti microalloy steel from both test methods b) Thermodynamic modeling showing precipitation of TiN along with (Nb,Ti,V)(C,N) formation after solidification from 600 -1100 °C.

TiN precipitates may pin the austenite grain boundaries, possibly preventing grain growth and improving ductility of the alloy comparing the other two steels [20]. However, TiN can also reduce the availability of nitrogen to form precipitates of AlN or Nb(C,N), which can be beneficial to the hot ductility of steel [19].

The reader should be reminded that the two test methods employed in these tests rely on the re-solutioning of precipitates during the sample soaking period prior to cooling to the test temperature. This treatment path cannot re-dissolve all of the expected precipitates, such as TiN and MnS, which can form at temperatures above our soaking temperature capabilities. In the proposed future in-situ bend tests, we hope to be able overcome this limitation and evaluate the importance of this difference on hot ductility test results.

Width of hot ductility trough

The position of the low temperature end of the ductility trough is closely related to the carbon content of the alloy. Among the three steels examined, V microalloy steel had the highest carbon content of 0.175 wt. %. Increasing the carbon level of the alloy shifts the γ → α phase transformation temperature (Ar$_3$) to lower temperatures. At still lower temperatures, all three steels exhibited higher ductility as the ferrite volume fraction increased. Mintz, et. al. reported that the main reason for the ductility improvement is a more even distribution of strain with increasing volume fractions of ferrite [15, 21]. At temperatures greater than 850°C, the three steels all showed an increase in ductility, with %RA's of around 98% in austenite. At the high temperature end of the ductility trough, the increased cooling rate used with the joule heating experiment also tended to measure a lower temperature for the top side of the ductility trough compared to the slower cooling rate MTS frame test. This difference is likely due to the effect that cooling rate has on temperature that ferrite nucleates. Ferrite nucleation occurs at lower temperatures as cooling rate increases.

Depth of hot ductility troughs

The hot ductility troughs from two testing methods for V microalloy steels are deeper and broader compared to other steels. This may be due to the formation of vanadium carbide precipitates in the ferrite films that form at 700-850°C as predicted by the thermodynamic modeling as shown in Figure 4(b) or the higher carbon content of this steel. In the Nb-Ti steel, the trough from the MTS load frame is narrower than joule heating, which appears to be wider. The difference in the shape of the trough from the two methods is likely caused by the difference in cooling rates of the test methods. The joule heating test was operated at a higher cooling rate than MTS load frame. The trough of the V-Nb-Ti microalloy steels from both test methods are narrower and more shallow compared to the other steels. This may be due to the formation of TiN precipitates which restricts grain growth and results in a finer grain size or from the scavenging of nitrogen. Metallographic and TEM analyses are planned in future work to investigate these observed differences in ductility.

Austenite Grain Size

Comparing the three steels in this study, Figure 9, the V microalloyed steel had a substantially larger average prior austenite grain size (208 μm) than the Nb -Ti and V-Nb-Ti steels (36 μm and 28 μm, respectively). The Ti added grades both exhibited a finer austenite grain size than the V microalloyed steel. When the temperature of the sample is decreased below the Ar$_3$ temperature, the austenite grain boundaries become covered with thin films of ferrite and with fine prior austenite grains, the ferrite distributes more uniformly, resulting in a more refined microstructure [18]. The V microalloyed steel has the coarsest grain size and also had the deepest and widest ductility trough along with the lowest %RA when compared to the other microalloyed steels. Steels with a finer the grain size are generally more resistant to crack propagation. With finer grain size, the aspect ratio of the crack which controls the stress concentration at the crack tip is reduced making it difficult for crack propagation [17]. Metallographic analysis and fractography investigations are planned in future work to investigate the mechanisms of fracture for these steels.

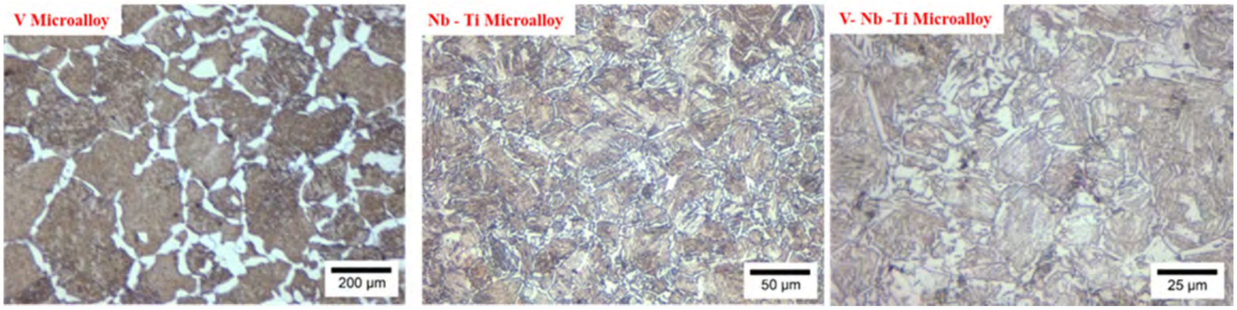

(a) (b) (c)

Figure 9. Prior austenite grain size analysis of as-cast a) V microalloy steel with an average grain size of 208 µm b) Nb -Ti microalloy steel with an average grain size of 36 µm and c) V-Nb-Ti microalloy with an average grain size of 28 µm. These steels were heat treated to form ferrite on the prior austenite grain boundaries to facilitate the austenite grain size measurements.

CONCLUSION

Hot ductility curves were obtained using two high temperature test methods: (1) a tensile test utilizing a servo-hydraulic load frame with a resistance furnace and (2) a thermomechanical testing apparatus using rapid joule heating combined with an electro-mechanically controlled tensioning system. Both test methods showed similar low ductility trends, but the upper and lower edges of the ductility trough differed somewhat between the two test methods. The differences are attributed to the differences in heating and cooling rate of the two test methods. The V micro alloyed steel slab sample had significantly lower ductility (40% RA) compared to the other two steels tested. The Nb-Ti and V-Nb-Ti microalloy steels displayed similar ductility minimums, and the temperature at which the minimum ductility was observed varied between 750-800°C. Both the Nb-Ti and V-Nb-Ti steels had improved ductility compared to V microalloy steels. V microalloy steel had the widest and deepest trough compared to other steels, but it also had the highest carbon content (0.17%C). The increased carbon shifts the ductility trough shifts to lower temperatures (750°C) due to the decrease in the $\gamma \rightarrow \alpha$ phase transformation temperature. Ductility loss in these steels may be largely controlled by the formation of thin films of ferrite at low temperatures, given that the measured low ductility temperature regions correlate well with the thermodynamically predicted $\gamma \rightarrow \alpha$ transformation temperatures. In future work, a test procedure that directly tests the as-solidified and cooled steel is planned to examine the importance of high temperature precipitates, such as TiN.

ACKNOWLEDGEMENT

The authors would like to thank United States Steel Cooperation for providing as-cast slab samples for hot ductility studies. Additionally, the authors would also like to acknowledge undergraduate research assistant Aileen Martinez for her contribution on the sample preparation. This project was supported by Peaslee Steel Manufacturing Research Center (PSMRC) at Missouri University of Science and Technology (Missouri S&T), thanks to all the faculties and industry mentoring committee of PSMRC for their help and guidance.

REFERENCES

1. H G Suzuki, S Nishimura, and S Yamaguchi, “Embrittlement of Steels Occurring in the Temperature Range from 1000-600 °C”, *Trans ISIJ,* Vol. 24, 1984, pp 169-174.

2. B Mintz, and J M Arrowsmith, “Hot ductility behavior of C-Mn-Nb-Al steels and its relationship to crack propagation during the straightening of continuously cast strand”, *Metals Technology*, Vol. 6, 1979, pp 24-32.

3. M. A. Matveev, "Causes of High Temperature Ductility Trough of Microalloyed Steels", *Trans Indian Inst Met,* Vol. 70, No.8, 2017, pp 2193-2204.
4. K R Carpenter, R Dippenaar and C R Killmore, "Hot Ductility of Nb- and Ti-Bearing Microalloyed Steels and the Influence of Thermal History", *Metallurgical and Materials Transactions A,* Vol. 40A, 2009, pp 573 – 580.
5. T Gladman: The Physical Metallurgy of Microalloyed Steels, Maney, London, 2002.
6. M P Rao, V S Sarma and S Sankaran," Development of high strength and ductile ultrafine grained dual phase steel with nano sized carbide precipitates in a V–Nb microalloyed steel", *Materials Science & Engineering A,* Vol. 568, 2013, pp 171-75.
7. E Peroloma ,I Timokina, K Russell and M Miller, "Characterization of clusters and ultrafine precipitates in Nb-containing C–Mn–Si steels", *Scripta Materialia,* Vol.54, 2006, pp 471–476.
8. B Patrick and V Ludlow, "Development of Casting Practices to Minimise Transverse Cracking in Microalloyed Steels", Revue de Metallurgie, Vol. 91, 1994, pp 1081-1089.
9. Yue Liu, Lin-Xiu Du, Hong Yan Wu and R Devesh Kumar Misra, "Hot ductility and Fracture Phenomena of Low-Carbon V-N-Cr Microalloyed Steels", *Steel Research International*, Vol. 91, 2020, pp 1- 11.
10. J R Wilcox and R W K Honeycombe, "Hot Ductility of Nb and Al Microalloyed Steels Following High Temperature Solution Treatment", *Metals Technology*, Vol. 11, 1984, pp 217-225.
11. C Ouchi and K Matsumoto, "Hot Ductility in Nb-bearing High Strength Low-alloy Steels", *Trans ISIJ*, Vol. 22, 1982, pp 181-189.
12. L Zhen, Z Hongtao, W Baorong, "Effect of Niobium on Hot Ductility of Low C-Mn Steel Under continuous Casting Simulation Conditions", *Steel Research*, Vol. 61, 1990, pp 620- 623.
13. P Sricharoenchai, C Nagasaki and J Kihara, "Hot Ductility of High Purity Steels Containing Niobium", *ISIJ International*, Vol. 32, 1992, pp 1102-1109.
14. B Mintz, "Hot Ductility of Steels and its Relationship to the Problem of Transverse cracking during continuous Casting", *International Materials Review*, Vol. 36, No.5, 1991, pp 187-217.
15. B Mintz, "The Influence of Composition on the Hot Ductility of Steels and to the Problem of Transverse Cracking" *ISIJ International*, Vol.39, 1999, pp 833-855.
16. B Mintz and J M Arrowsmith, "Influence of Microalloying Additions on Hot Ductility of Steels", in "Hot Working and Forming Processes", *The Metals Society*, 1980, pp 99-103.
17. D N Crowther and B Mintz, "Influence of grain size on hot ductility of plain C-Mn steels", *Materials Science and Technology*, Vol. 2 No. 9, 1986, pp 951-955.
18. U H Lee, T E park, K S Son, M S Kang, Y M Won, C H Yim, S K Lee, I Kim and D Kim, " Assessment of hot ductility with various thermal histories as an alternative method of in situ solidification, *ISIJ International*, Vol. 50, No. 4, pp.540-545.
19. K R Carpenter, "The influence of microalloying elements on the hot ductility of thin slab cast steel", University of Wollonglong, *PhD Thesis*, 2004
20. R Abushosha, O Comineli and B Mintz, "Influence of Ti on hot ductility of C-Mn-Al steels", *Material Science and Technology*, Vol.15, 1999, pp 278 – 286.
21. A Cowley, R Abushosha and B Mintz, "The influence of Ar_3 and Ae_3 temperatures on the hot ductility of steels", *Material Science and Technology*, Vol. 15, 1998, pp1145-1153.